Internal Strain Measurement by Neutron Diffraction Under Transverse Compressive Stress for Nb_3Sn Wires With and Without Cu-Nb Reinforcement

Mio Nakamoto, Michinaka Sugano, Toru Ogitsu, Masahiro Sugimoto, Ryo Taniguchi, Kiyoshige Hirose, Takuro Kawasaki, Wu Gon, Stefanus Harjo, Satoshi Awaji, and Hidetoshi Oguro

***Abstract*—For an accelerator magnet, a certain mechanical strength is required to sustain against a transverse compression stress due to Lorentz force. A bronze-route Nb_3Sn wire with Cu-Nb reinforcement was developed by Tohoku University and Furukawa Electric to enhance the strength against axial tension. The Cu-Nb reinforcement wire also exhibited some indication of strength improvement against transverse compression; however, the details of a reinforcement mechanism for the transverse compression stress have not been clarified. In this study, the internal strains of Nb_3Sn bronze-route wires with and without the Cu-Nb reinforcement under transverse compression stress were evaluated by neutron diffraction at BL19 (TAKUMI) in J-PARC. The samples were attached to jig with solder only at the ends and compression was applied at the center of the samples with 30-mm anvil with 5-mm wide and 8- to 15-mm high beam. Since a critical current, I_c of a superconducting wire depends on the three-dimensional strain, internal strain of Nb_3Sn along the axial and two orthogonal radial directions were evaluated at room temperature (RT). In the different setup, I_c measurements of the wires under transverse compression stresses were also performed at 4.2 K and 14.5 T. Using 3-mm wide anvil, the transverse compression was applied at 4.2 K or RT. The neutron diffraction results indicated no significant differences in the internal strains of Nb_3Sn under transverse compression between the samples with and without Cu-Nb reinforcement, while the I_c measurements showed potential increase in the irreversible stress (σ_{irr}) for Cu-Nb reinforced wires. The reason for this discrepancy was discussed based on the difference in the experimental setups for each measurement.**

***Index Terms*—Bronze-route wire, critical current, internal strain, neutron diffraction, Nb_3Sn.**

Manuscript received 26 September 2023; revised 6 February 2024; accepted 6 March 2024. Date of publication 19 March 2024; date of current version 9 April 2024. This work was supported by Grants-in-Aid for Scientific Research B under Grant 23H01190. *(Corresponding author: Mio Nakamoto.)*

Mio Nakamoto is with the Graduate University for Advanced Studies (SOKENDAI), Tsukuba 305-0801, Japan, and also with the National Institutes for Quantum Science and Technology, Naka 311-0193, Japan (e-mail: nakamoto.mio@qst.go.jp).

Michinaka Sugano and Toru Ogitsu are with the High Energy Accelerator Research Organization (KEK), Tsukuba 305-0801, Japan.

Masahiro Sugimoto, Ryo Taniguchi, and Kiyoshige Hirose are with the Furukawa Electric, Nikko 321-1493, Japan.

Takuro Kawasaki, Wu Gon, and Stefanus Harjo are with the Japan Atomic Energy Agency, Tokai 319-1195, Japan.

Satoshi Awaji is with the Tohoku University, Sendai 980-8577, Japan.

Hidetoshi Oguro is with the Tokai University, Hiratsuka 259-1207, Japan.

Color versions of one or more figures in this article are available at https://doi.org/10.1109/TASC.2024.3379124.

Digital Object Identifier 10.1109/TASC.2024.3379124

I. Introduction

FOR the Future Circular Collider (FCC), Lorentz force will exert some axial strain up to ±0.3% and some transverse compression up to 200 MPa on the magnets at the design field of 16 T [1], [2]. An application of Nb_3Sn conductors for their high field magnets is under consideration. Therefore, the magnets should sustain those severe mechanical conditions, regardless of the brittleness of Nb_3Sn. To overcome this challenge, some global R&D for magnet design and development of conductors is ongoing [3]. The development target for Nb_3Sn conductor wire was set to a non-Cu current density (J_c) of 1, 500 A/mm^2 at 16 T and 4.2 K. Currently, the Restacked Rod Process (RRP) wire developed by Oxford Superconducting Technology is one of the most promising wires with the best J_c achieved, 1, 300 A/mm^2 [4]. The R&D within the framework of CERN-KEK collaboration is also conducted in Japan and 1, 100 A/mm^2 has been achieved by a distributed tin wire manufactured by JASTEC [5]. The former is reported to exhibit I_c reduction at 145–175 MPa [6] while the latter showed some irreversible discontinuous degradation around 125 to 150 MPa [7]. Further enhancements against transverse compression stresses are necessary.

In 25 T Cryogen-free superconducting magnet project at Tohoku University, a bronze-route Nb_3Sn superconducting wire with a Cu-Nb reinforcement was developed [8]. In this wire, Cu-Nb is added to the stabilizer copper as shown in Fig. 1. The fine Nb filaments in the Cu-Nb layer act as fiber reinforcement. This wire was developed to sustain the axial tensile stress of 350 MPa and transverse compressive stress of 60 MPa at 14.5 T, 4.2 K and those targets have been satisfied [9], [10]. The report showed a potential improvement in I_c reduction by addition of the Cu-Nb reinforcement. Since this is a bronze-route wire, its current density, J_c is too low to be used for an accelerator magnet. However, the concept of a Cu-Nb reinforcement may be applicable to accelerator magnet wires if it improves the transverse mechanical strength to the development target.

To understand the strengthening mechanism of Cu-Nb reinforcement, the study of the internal strains of wires with Cu-Nb reinforcement was necessary. Due to its long penetration depth, neutron diffraction experiments are often practiced for internal strain measurements for superconducting magnet wires or cables

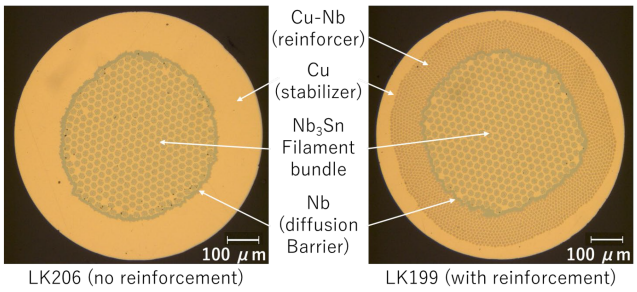

Fig. 1. Bronze route Nb_3Sn wires with or without Cu-Nb reinforcement.

TABLE I
SPECIFICATIONS OF Nb_3Sn WIRES WITH OR WITHOUT CU-NB REINFORCEMENT

Type	LK199	LK206
Heat treatment condition	670℃x96h	670℃x96h
Wire diameter (mm)	0.8	0.8
Twist pitch (mm)	24	24
Nb filament diameter (μm)	3.2	3.2
Non-Cu/Cu/Cu-Nb fraction (%)	45/20/35	45/55/0

[11], as well as impregnated samples [12], [13] under axial or transverse strains.

In this study, observations of the internal strains of Nb_3Sn wires under the transverse compression stress were conducted by neutron diffraction experiments. Since a critical current, I_c of a superconducting wire depends on the three-dimensional strain [14], the internal strain observations were performed in three directions. To understand the Cu-Nb enhancement mechanism, the measurements were performed on the samples with or without Cu-Nb reinforcement. The I_c measurements under transverse compression stress were also conducted and the results were compared against the neutron diffraction results.

II. EXPERIMENTAL DETAILS

The specifications of two types of wires are summarized in Table I. Both are bronze-route wires of 0.8 mm in diameter manufactured by Furukawa Electric. One with a Cu-Nb reinforcement is called LK199 while the other is LK206.

A. I_c Measurements With Transverse Compression Stresses at RT and 4.2 K

The I_c measurements were conducted for cases with transverse compressions applied at room temperature (RT) and at low temperature (4.2 K). The measurements were taken using the transverse load probe [7] and the 18-T solenoid magnet at Tohoku University.

For RT compression application, the target load was applied to each sample with the compression load probe and completely removed before insertion into the 18-T magnet. Then the probe was inserted into the magnet for I_c measurement in liquid helium at 14.5 T. After the I_c measurement, the probe was extracted from the magnet to replace the sample for the next measurement. Each sample was only used for one compression stress value since the sample would experience additional thermal cycles if reused.

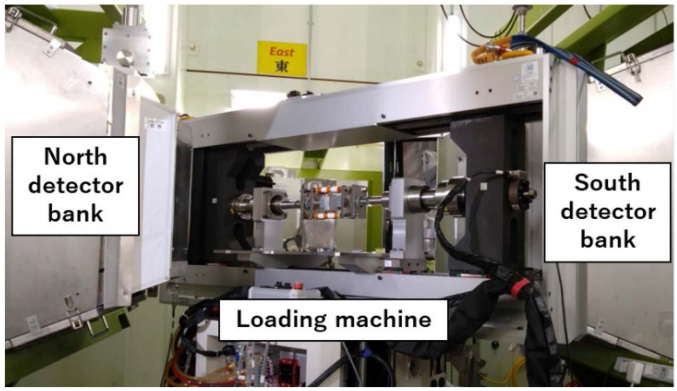

Fig. 2. Neutron diffraction measurements at J-PARC TAKUMI.

For the low temperature (4.2 K) compression application, target loads were applied after the insertion of the transverse load probe into the 18-T magnet. For each sample, the load was increased by 10 N (4.2 MPa) steps under 14.5 T for I_c measurements under loads (under-load measurements), then at every step, load was removed fully to check the reversibility of I_c (unloaded measurements).

The applied stress was calculated by dividing the applied load by the product of the anvil width of the transverse load probe, 3 mm, and the wire diameter of the sample, 0.8 mm.

I_c was taken by recording the inter-tap voltage response to a ramping applied current at 14.5 T in liquid helium at 4.2 K. The evaluation of I_c was based on an electric field criterion (E_c) of 1 μV/cm in this experiment.

B. Neutron Diffraction Experiments

Neutron diffraction was chosen as the method to observe the internal strains of samples under transverse compression since a neutron beam can penetrate through 30 to 40 mm thick materials while an application of compression up to 300 or 400 MPa requires bulky jigs for the experiment. The diffractions were taken by TAKUMI, a time-of-fight (TOF) neutron diffractometer installed at the beamline 19 in Materials and Life Science Experimental Facility (MLF) / Japan Proton Accelerator Research Complex (J-PARC) (Fig. 2). Pulsed neutron beams with a repetition rate of 25 Hz were introduced to the specimen [15]. The beam used in the experiment is a white neutron beam with multiple wavelengths; therefore, multiple diffraction peaks can be observed simultaneously. The beam, 5 mm wide and 8 to 15 mm high, is focused on the center of the samples. This instrument exhibits a machine resolution of better than 0.2% which corresponds to the experimental resolution of 5×10^{-3}% [16].

The internal strain of a wire under transverse compression stress can be obtained as a sum of the initial residual strain and the internal strain change due to the compression. The neutron diffractions were taken for both sample types in different conditions as summarized in Table II, 1) samples on compression jigs

TABLE II
SUMMARY OF NEUTRON DIFFRACTION CONDITIONS

Setup		Soldered wire	Free wire	Filament
RT compression	RT	done	N.A.	done
Low temperature setup	RT	N.A.	done	done
Low temperature setup	13 K	N.A.	done	done

to evaluate the internal strains under the transverse compression stresses, 2) the Nb_3Sn filaments extracted from the composite wires by a chemical etching to observe the lattice spacings of Nb_3Sn in strain-free state, and 3) free-wire samples to observe the residual internal strains.

Experimental setups were designed for RT and at low temperature. Diffractions for the Nb_3Sn filaments and the free wire samples were taken at both RT and 13 K, the lowest reachable temperature with the cryogenic cooling system. The low temperature setup is used for measurements of residual strains. The Nb_3Sn filaments were packed in polyimide or vanadium tubes. For the free wire samples, eight short wires for each wire type were attached to an aluminum plate with an aluminum tape. Both were installed on the second stage of the GM cooler during the measurements.

Diffractions for samples on compression jigs were only taken at RT. Aluminum alloy was chosen as compression jig material since aluminum has high transmittance for neutron beam (~40 mm) and any of its peaks do not overlap with Nb_3Sn peak. Also, it has good thermal conductivity and is convenient for future low temperature experiments. For each set, four 60-mm long samples were attached to the sample holder of the compression jig by soldering the two ends to copper terminals. The soldering of the two ends was done to match the constraint conditions of the samples to that of the I_c measurements. Then the compression jig with 30 mm contact length will apply the compression when a loading machine is set to motion.

A loading machine capable of applying 50 kN was installed on the goniometer for the transverse compression application (Fig. 2). The compression load was applied in stepwise process. Data was taken with the same load pattern as the RT I_c measurements. At each step, a sufficient duration was given to accumulate data of neutron diffractions and the data was compiled for analysis. To obtain the internal strains in three orthogonal directions, experiments were conducted with samples oriented in horizontal and vertical directions (Fig. 3). In both horizontal and vertical arrangements, diffraction beams from compression direction were observed by North detector bank (RC1 and RC2). The comparison of those data showed the validity of the data obtained from the experiments. With the South detector bank, diffraction beams from axial direction (Axial) and radial direction perpendicular to compression (RP) were observed in horizontal and vertical arrangements, respectively.

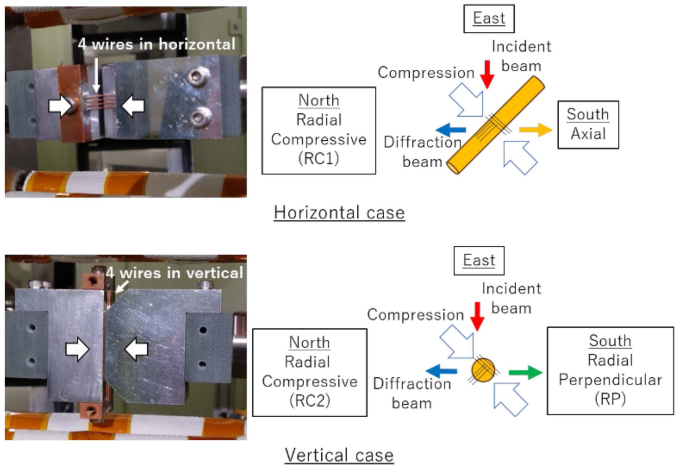

Fig. 3. Transverse compression application with the loading machine.

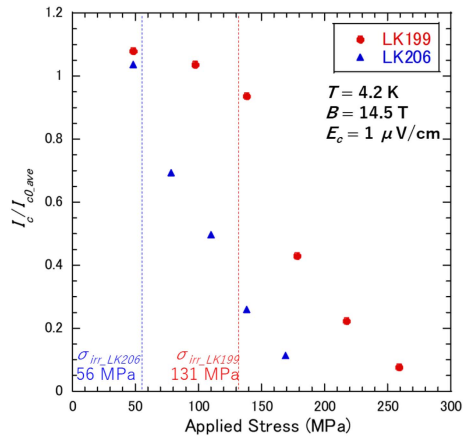

Fig. 4. Normalized I_c after application of transverse compression stress at room temperature.

III. I_c MEASUREMENT RESULTS

A. *Effect of RT Transverse Compression on I_c*

The normalized I_c values with respect to applied stresses at RT are shown in Fig. 4. The normalization of I_c is done with reference to the average initial I_c values, before application of stresses, obtained for the samples for low temperature measurements (I_{c0_ave}) in Fig. 5 for each kind. Here, the irreversible stress (σ_{irr}) was defined as the stress limit where I_c of unloaded measurement takes 95% of I_{c0_ave} value and determined by the linear interpolation from the closest two points. For LK199 with Cu-Nb reinforcement, the σ_{irr} value was 131 MPa, while the value was 56 MPa for LK206 without Cu-Nb reinforcement. The results indicate that the I_c of unloaded measurement starts to degrade at higher transverse compression stress for a wire with Cu-Nb reinforcement at RT.

B. *Effect of Transverse Compression at 4.2K on I_c*

The normalized I_c values with respect to the transverse compressive stresses applied at 4.2 K are plotted in Fig. 5. The I_c is normalized to the initial value of I_c for each sample, I_{c0}. The solid symbols and the open symbols in the figure indicate the

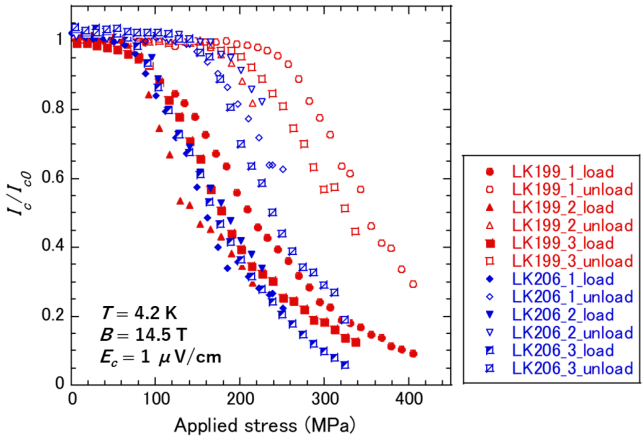

Fig. 5. Normalized I_c under transverse compression stress at low temperature.

TABLE III
SUMMARY OF STRESS, σ (MPA) AT $I_c = 95\%$ OF I_{c0}

Sample	LK199		LK206	
Conditions	Under-load	Unloaded	Under-load	Unloaded
RT	N.A.	131	N.A.	56
LT_1	98	248	78	153
LT_2	78	182	96	188
LT_3	81	204	87	165
LT_average	86	211	87	169
LT_std	11	33	9	18

under-load and the unloaded measurement data, respectively. For better visualization, the unloaded measurement data is plotted over the maximum stress applied before unloading. The compressive stress values at which the I_c reaches 95% of I_{c0} are summarized in Table III for both under-load and unloaded cases.

The degradation of I_c begins at where stress is concentrated, resulting in the larger standard deviation. For under-load cases, stress is low and Nb_3Sn filaments are still in the elastic state when I_c is 95% of I_{c0}. For unloaded case at 4.2 K, the trends of the n-values from V-I curve imply the occurrence of fractures in Nb_3Sn filaments near σ_{irr}. Since a fracture in filament often begins at the location of stress concentration and the maximum experienced stresses are higher for LK199 than LK206, the impact of stress concentration appears more prominently on the stress where fracture begins. From those reasons, the larger standard deviations would occur in σ_{irr} for LK199. This effect of stress concentration at the edge of anvil will be verified through additional experiments under contemplation.

In the previous study [10], the reduction of I_c under the transverse compression at 4.2 K and 14.5 T were observed for the same types of wires; however, with pre-bending treatment. In this study, the samples were as-reacted wires; and the results cannot be directly compared. It should be also noted that in this study, the stress is directly applied on the single wires to compare the impact on Nb_3Sn wires with and without Cu-Nb reinforcement. However, in the magnet, Nb_3Sn cables are impregnated with resins, in the different constraint conditions, and a change in I_c of Nb_3Sn under transverse compressive stress is much more marginal [17].

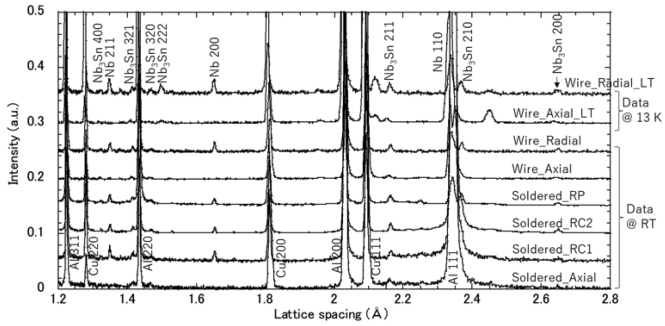

Fig. 6. Diffraction pattern of Cu-Nb reinforced Nb_3Sn wire at room temperature.

IV. NEUTRON DIFFRACTION RESULTS

The diffraction patterns were fitted at the target peak position with Voigt function to evaluate the peak locations. The peak location directly translated into the lattice spacing. Nb_3Sn peak 211 was selected to study since it does not overlap with other peaks and is relatively easier to fit. The examples of diffraction patterns are shown in Fig. 6. In our experiment, a pure copper peak cannot be distinguished from a bronze alloy peak; however, the peak is indicated as "Cu" in Fig. 6. Moreover, even though peaks for copper and niobium are visible, they are not discussed in this study since the focus of our discussion is on the strain status of Nb_3Sn. The diffraction patterns indicated as 'Wire' are for free wire samples and ones with 'Soldered' are the data taken with soldered samples on the aluminum compression jig before application of any compression.

As already mentioned, the internal strain of a wire under transverse compression stress can be obtained as a sum of the initial residual strain and the internal strain change due to the compression. From the lattice spacings of Nb_3Sn 211, an internal strain ε_i and a residual strain ε_r can be expressed as (1) and (2), respectively.

$$\varepsilon_i\ (\sigma,\ T) = \varepsilon_r\ (T) + \varepsilon_i^{Rel}\ (\sigma,\ T)\,,\ \text{and} \tag{1}$$

$$\varepsilon_r\ (T) = \frac{d\,(\sigma = 0,\ T) - d_0\,(T)}{d_0\,(T)},\ \text{where} \tag{2}$$

ε_i^{Rel} is the relative internal strain while d and d_0 are the lattice spacings for the peak of the interest and the strain-free state. Here, the negative strain means compression while the positive strain means tensile strain.

A. Residual Internal Strains

The residual strains calculated from the neutron diffraction experiments are summarized in Table IV. For free wires, 0.1 to 0.2% larger axial strain values were obtained for LK199 compared to LK206, while radial strain values did not show large differences. In I_c measurements, this increase in the axial strain due to addition of Nb filaments in stabilizer for LK199 Cu-Nb reinforcement wire did not show a largely impact on the

TABLE IV
SUMMARY OF RESIDUAL STRAINS

Wire type	Sample type	Temp.	Radial(%) RC1	RC2	RP	Axial(%)
LK199	Free wires	RT		0.02		-0.21
	Free wires	13 K		0.13		-0.34
	Soldered samples	RT	0.07	0.03	0.00	-0.07
LK206	Free wires	RT		0.01		-0.10
	Free wires	13 K		0.09		-0.17
	Soldered samples	RT	0.05	0.06	0.02	-0.06

I_c of the wires. The I_{c0} values decreased slightly by the addition of Nb filament, in average of 6.6%. The absolute values of the axial residual strains are equivalent to the results obtained in the previous study at both RT and low temperature [11].

For the soldered samples, the residual strain values obtained did not show any difference between the two types in any directions. The results do not agree to the results of free-wire samples. Since there would be the influences of soldering or the handling of jig installations, the residual strains of free-wire samples will be used for comparison with the neutron diffraction results.

B. Transverse Compression Dependencies of Internal Strains at RT

The changes in internal strain conditions with increasing stress can be observed from the relative internal strains obtained at RT for both LK199 and LK206 in Fig. 7. A relative strain of Nb_3Sn at RT can be calculated as in (3).

$$\varepsilon_i^{Rel}\ (\sigma,\ RT) = \frac{d\,(\sigma,\ RT) - d\,(\sigma = 0,\ RT)}{d\,(\sigma = 0,\ RT)} \tag{3}$$

The evaluation results of under-load and unloaded cases are shown in Fig. 7(a) and (b), respectively. For under-load cases, the increase in transverse compressive stress exerts compressive strains in the compression direction (RC1 and RC2) and tensile strains in the direction perpendicular to compression (RP). The absolute values are not so different in the compression direction and perpendicular to the compression direction; however, the signs are opposite. The internal strains change linearly up to 180 MPa, and above that stress, the change becomes nonlinear. No significant differences between LK199 and LK206 appear; however, the data is only taken in the linear range for LK206. The axial strain values are much smaller compared to radial directions and no differences between the two wire types were indicated.

For unloaded cases, the values are small but compressive strains remain in the compression direction and tensile strains remain in the radial direction perpendicular to compression. Even after compression stresses are released, some strains remain by the plastic deformation of the wires. However, no large difference between LK199 and LK206 was observed.

When a transverse compression stress is applied to a wire, strain distribution appears in the wire [14]. To study if any

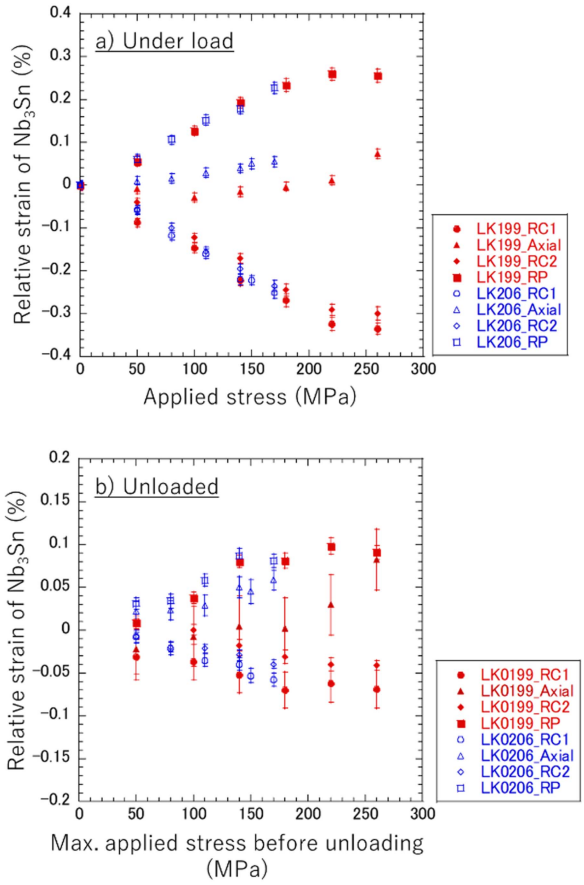

Fig. 7. Applied stress dependency of relative internal strains at room temperature for (a) under-load, and (b) unloaded cases.

differences exist in the strain distributions of LK199 and LK206, the change in the FWHM under transverse compression stresses was also observed. Fig. 8(a) and (b) each shows the change in FWHM of the Nb_3Sn 211 for under-load and unloaded cases. The irreversible strain limits obtained from the RT I_c measurements are indicated with a dotted line in Fig. 8. The broadening of a peak in compression direction for LK199 (LK199_RC1 and RC2) occurs at irreversible strain; however, such transition could not be recognized for LK206. Also, no significant differences are manifested between LK199 and LK206 in FWHM trends, either.

The neutron diffraction experiment results are compared against the I_c measurement result. The internal strain values obtained from the neutron diffraction experiments were the same for LK199 and LK206 in all cases. This is the same outcome for under-load results of the I_c measurements at low temperature. However, for the unloaded cases, the I_c starts to degrade at much higher stresses for LK199 than LK206 at both RT and the low temperature. These outcomes are not consistent with the neutron diffraction results.

One of the reasons for this inconsistency is the edge effect of the anvil. During the neutron diffraction experiments, the compression stress is applied over the 30 mm range and the neutron beam is focused at 5 to 15 mm ranges at the center of the compression; therefore, the edge effect is not observed.

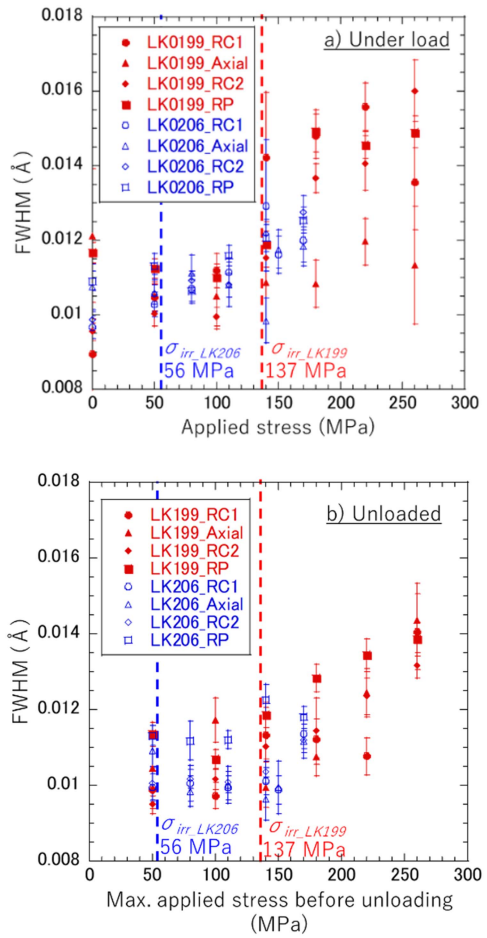

Fig. 8. Applied stress dependency of FWHM at room temperature for (a) under-load and (b) unloaded cases.

On the other hand, in the I_c measurements, the transverse compression stress is applied with a 3-mm wide anvil and the voltage tap wires are attached at 10 mm distance over the compression range; thus, the edges of the compression are in the measurement range. If there are stress concentrations on the wires in contact with the edges, there is a possibility that the impact of plastic deformations in those regions appear more distinctively under-load cases. Further study with I_c and mechanical strain measurements on samples mocking up the compression condition of the neutron diffraction experiments is planned to clarify this matter.

V. Conclusion

The neutron diffraction experiments were conducted on bronze-route wires with or without a Cu-Nb reinforcement. The residual strains and three-dimensional strain changes were successfully observed under transverse compression stresses. Regarding the residual strains, 0.1% strain differences were observed between the two types of the wires in axial direction at RT; however, no significant differences in radial directions were observed. The changes in internal strains under transverse compressive stresses showed no differences regardless of under-load or unloaded. In the I_c measurement, no significant differences were found in the low temperature under-load cases; however, the I_c of under-unload case starts to degrade at the higher transverse compressive stresses for Cu-Nb reinforced wires in both RT and low temperature conditions. To reveal the dependence of the I_c on the transverse compressive stresses for those wires, which is present in magnet operation, further experiments taking consideration of the differences in anvil structures used in the two experiments will be conducted to eliminate the edge effect of the anvil.

Acknowledgment

The neutron experiment at the Materials and Life Science Experimental Facility of the J-PARC was performed under a user program Proposal No. 2022B0213 and 2023A0254. The high magnetic field measurements were performed at HFLSM, IMR, Tohoku University.

References

[1] A. Ballarino and L. Bottura, "Targets for R&D on Nb_3Sn conductor for high energy physics," *IEEE Trans. Appl. Supercond.*, vol. 25, no. 3, Jun. 2015, Art. no. 6000906.
[2] V. Marinozzi et al., "Conceptual design of a 16 T cos θ bending dipole for the future circular collider," *IEEE Trans. Appl. Supercond.*, vol. 28, no. 3, Apr. 2018, Art. no. 4004205.
[3] A. Ballarino et al., "The CERN FCC conductor development program: A worldwide effort for the future generation of high field magnets," *IEEE Trans. Appl. Supercond.*, vol. 29, no. 5, Aug. 2019, Art. no. 6000709.
[4] C. Sanabria et al., "Controlling Cu-Sn mixing so as to enable higher critical current densities in RRP Nb_3Sn wires," *Supercond. Sci. Technol.*, vol. 31, 2018, Art. no. 064001.
[5] S. Kawashima et al., "Development of high current density distributed tin method Nb_3Sn wire," *IEEE Trans. Appl. Supercond.*, vol. 30, no. 1, Jan. 2020, Art. no. 6000105.
[6] J. F. Troitino et al., "Effects of the initial axial strain state on the response to transverse stress of high-performance RRP Nb_3Sn wires," *Supercond. Sci. Technol.*, vol. 34, Jan. 2021, Art. no. 035008.
[7] M. Nakamoto et al., "Influence of axial strain and transverse compressive load on critical current of Nb_3Sn wires for the FCC," *IEEE Trans. Appl. Supercond.*, vol. 33, no. 5, Aug. 2023, Art. no. 8400505.
[8] S. Awaji et al., "New 25 T cryogen-free superconducting magnet project at Tohoku university," *IEEE Trans. Appl. Supercond.*, vol. 24, no. 3, Jun. 2014, Art. no. 4302005.
[9] M. Sugimoto et al., "Development of Nb-rod-method Cu-Nb reinforced Nb_3Sn Rutherford cables for react-and-wind processed wide-bore high magnetic field coils," *IEEE Trans. Appl. Supercond.*, vol. 25, no. 3, Jun. 2015, Art. no. 6000605.
[10] M. Sugimoto et al., "Evaluation of various Nb-rod-method Cu-Nb/Nb_3Sn wires designed for practical react-and-wind coils," *IEEE Trans. Appl. Supercond.*, vol. 30, no. 4, Jun. 2020, Art. no. 6000905.
[11] K. Takahashi et al., "Internal strain measurement for a Nb_3Sn Rutherford cable using neutron diffraction," *IEEE Trans. Appl. Supercond.*, vol. 25, no. 3, Jun. 2015, Art. no. 8400104.
[12] F. Wolf et al., "Effect of applied compressive stress and impregnation material on internal strain and stress state in Nb_3Sn Rutherford cable stacks," *IEEE Trans. Appl. Supercond.*, vol. 29, no. 5, Aug. 2019, Art. no. 8400605.
[13] C. Scheuerlein et al., "Direct measurement of Nb_3Sn filament loading strain and stress in accelerator magnet coil segments," *Supercond. Sci. Technol.*, vol. 32, 2019, Art. no. 045011.
[14] C. Calzolaio et al., "Electro-mechanical properties of PIT Nb_3Sn wires under transverse stress: Experimental results and FEM analysis," *Supercond. Sci. Technol.*, vol. 28, Apr. 2015, Art. no. 055014.
[15] K. Nakajima et al., "Materials and life science experimental facility (MLF) at the Japan proton accelerator research complex II: Neutron scattering instruments," *Quantum Beam Sci.*, vol. 1, no. 3, Nov. 2017, Art. no. 9.
[16] S. Harjo et al., "Current status of engineering materials diffractometer at J-PARC," *Mater. Sci. Forum*, vol. 681, pp. 443–448, 2011.
[17] G. Mondonice et al., "Effect of quasi-hydrostatical radial pressure on I_c of Nb_3Sn wires," *Supercond. Sci. Technol.*, vol. 25, 2012, Art. no. 115002.